Optical vortex coronagraph

Gregory Foo, David M. Palacios, and Grover A. Swartzlander, Jr.

College of Optical Sciences, University of Arizona, Tucson, Arizona 85721

Received July 18, 2005; accepted August 4, 2005

We describe a method to observe dim exoplanets that eliminates light from the parent star across the entire exit pupil without sacrificing light from the planet by use of a vortex mask of topological charge $m=2$.

OCIS codes: 110.6770, 070.6110, 350.1260.

The search for extrasolar planets is hampered by inadequate means of removing glaring starlight while leaving the planet light intact. This is a challenging optical design problem because the starlight is typically more than 10 million times brighter than the planet. Various coronagraph designs have been proposed to preferentially obstruct starlight.[1] For example, a nulling coronagraph[2,3] uses a mask to shift the phase over some region of the Airy disk of the star in an intermediate focal plane. Another approach employs a four-quadrant phase mask.[4] The proposed vortex coronagraph is a nulling coronagraph using a helical phase mask. Ignoring scattering and aberrations, we prove that a vortex coronagraph may extinguish any magnitude of starlight without attenuating the signal from a resolvable planet. This technique is useful for both nearly resolved and well-resolved systems, it requires neither complex motion nor interferometric stability, and it is suitable for space-based telescopes operating in any region of the spectrum. Other uses of the scheme include searches for zodiacal dust and controlling glare from a bright point source.

The design of a coronagraph[5–7] is depicted in Fig. 1. The entrance pupil (PP1) is established by the objective lens. To create an artificial solar eclipse in the image plane (FP3), Lyot's design[5] included an occulting mask (OM) in the first focal plane (FP1) to block the central image and an aperture ("Lyot stop") in the second pupil plane (PP2) to mask diffracted light from the OM. We propose replacing the OM with a vortex phase mask (VPM). Optical vortex spatial filtering was predicted and experimentally observed in 1992.[8] Recent applications for astronomical[9] and nonastronomical purposes[10,11] have been reported.

An optical vortex is characterized by a helical phase front in an electric field propagating along the z axis. In cylindrical coordinates the instantaneous field may be expressed as[12,13]

$$E(r',\theta',z) = g(r',z)\exp(\mathrm{im}\,\theta')\exp(-ikz), \qquad (1)$$

where $g(r',z)$ is a circularly symmetric field amplitude, $k=2\pi/\lambda$ is the wavenumber, λ is the wavelength of light, and m is an integer called the topological charge. The intensity profile of a diffracted vortex beam, depicted in Fig. 2(a), is characterized by a dark central hole and annular rings. A VPM [see Fig. 2(b)] may be used to transform a planar wavefront into a helical one.[14] Eighty-step VPMs have recently been made,[15] and nearly continuous helical surfaces are expected soon.[16,17]

A coronagraph is composed of three Fourier transforming lenses, L_1, L_2, and L_3, as shown in Fig. 1. To analyze the system for use in extrasolar planet detection, the existence of two barely resolvable point sources at infinity is assumed. The initial plane waves at PP1 may be written: $U_j(x,y)=A_j\exp(ik_{x,j}x)$, where $j=1,2$, A_j^2 is the intensity, and (in the paraxial approximation) the transverse wave vector has a magnitude $k_{x,j}\approx k\alpha_j$. The angle at which the star ($j=1$) subtends the optical axis is set to $\alpha_1=0$. We assume that the light sources are quasi-monochromatic and mutually incoherent and that the lenses are lossless, nonscattering, and aberration free. The radius of the entrance pupil is R_{EP} and all lenses have identical focal lengths f. In the plane FP1, having transverse coordinates (u,v), the transmitted fields may be written as[18]

$$U_j(u,v) = t(\rho,\theta)(i\lambda f)^{-1}\exp(ik\rho^2/2f)\int\int_{\mathrm{PP1}} P(x,y)U_j(x,y) \times\exp[-i(xu+yv)k/f]\mathrm{d}x\mathrm{d}y, \qquad (2)$$

where $P(x,y)$ is the entrance pupil function, defined as unity for $r=\sqrt{x^2+y^2}<R_{\mathrm{EP}}$ and zero otherwise. The integration in Eq. (2) is performed over this pupil. The OM for Lyot's coronagraph has a transmission function $t(\rho,\theta)=t_{\mathrm{OM}}(\rho)$ whose value is zero within a radius $\rho=\sqrt{u^2+v^2}<R_{\mathrm{OM}}$ and unity otherwise. The transmission of an VPM is given by $t(\rho,\theta)=t_{\mathrm{VC}}(\theta)=\exp(im\theta)$. We note that $U_2(u,v)$, whose centroid ap-

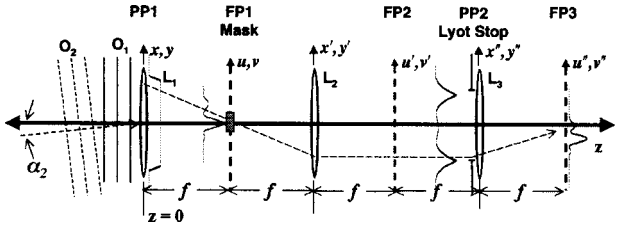

Fig. 1. Schematic of a coronagraph composed of lenses L_1, L_2, and L_3 of focal lengths f. The pupil planes PP and focal planes FP are shown with their respective coordinates. Spatial filtering by the mask in FP1 extinguishes light from the on-axis source (O_1) but transmits light from the off-axis source (O_2). Residual on-axis intensity appears near the perimeter of PP2, where it is truncated with a Lyot stop.

0146-9592/05/243308-3/$15.00

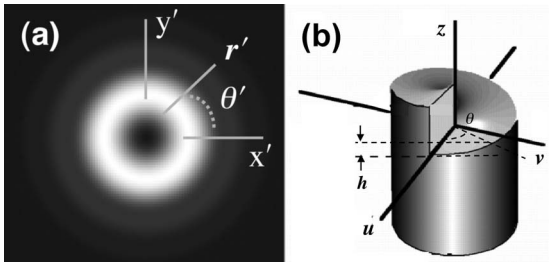

Fig. 2. (a) Intensity profile, $|U(x',y')|^2$ of a beam containing an optical vortex. (b) Surface profile of a VPM.

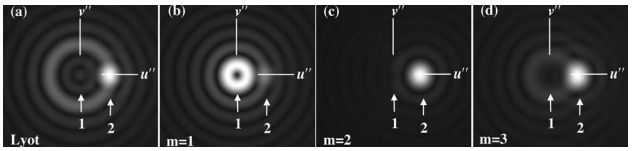

Fig. 3. Comparisons for $\alpha_2=\alpha_{\text{diff}}$ and $A_1^2/A_2^2=100$. (a) Lyot coronagraph where $R_{\text{OM}}=r_{\text{diff}}$. (b), (c), (d) Vortex coronagraphs where $m=1$, $m=2$, $m=3$, respectively. In (c) the starlight is essentially eliminated, revealing a high-contrast image of the planet when $m=2$.

pears at $u=f\alpha_2$, is relatively unaffected by the vortex mask when $\alpha_2 \geqslant \alpha_{\text{diff}}=0.61\lambda/R_{\text{EP}}$. Lens L_2 performs an inverse Fourier transform upon $U_j(u,v)$, thereby producing a filtered version of the initial planar fields in plane FP2:

$$U_j(u',v') = (i\lambda f)^{-1} \int\int_{\text{FP1}} U_j(u,v) \times \exp[i(u'u+v'v)k/f]\,\mathrm{d}u\,\mathrm{d}v. \quad (3)$$

The Lyot stop could be placed in plane FP2, but the beam is collimated between L_2 and L_3, and it is often practical to place it in plane PP2. Lens L_3 performs a Fourier transform upon the fields in FP2, thereby producing the imaged fields in plane FP3:

$$U_j(u'',v'') = (i\lambda f)^{-1} \int\int_{\text{PP2}} U_j(u',v') P_{\text{Lyot}}(u',v') \times \exp[-i(u'u''+v'v'')k/f]\,\mathrm{d}u'\,\mathrm{d}v'. \quad (4)$$

The Lyot stop has a transmission function $P_{\text{Lyot}}(u',v')=1$ for $\rho'=\sqrt{u'^2+v'^2}<R_{\text{Lyot}}$ and zero otherwise.

To demonstrate the superior performance of the vortex coronagraph over the occulting Lyot configuration, we first examine two barely resolvable sources where $\alpha_1=0$, and $\alpha_2=\alpha_{\text{diff}}=0.61\lambda/R_{\text{EP}}$. The field of the two mutually incoherent sources was computed with a fast Fourier transform algorithm on an $N\times N=2048\times 2048$ computational grid. Soft apertures (e.g., hyper-Gaussian functions of order 10) were used to obviate noise attributed to high spatial frequencies. Further, the mask function in plane FP1 was multiplied by $\cos^2(\pi x/N)\cos^2(\pi y/N)$ to truncate high spatial frequency noise. The optical design parameters were $\lambda=0.5$ μm, $f=50$ mm, $R_{\text{EP}}=12.5$ mm, $R_{\text{Lyot}}=0.9\,R_{\text{EP}}$, $R_{\text{OM}}=r_{\text{diff}}=f\alpha_{\text{diff}}$, and $A_1^2/A_2^2=100$. The image in FP3 for the Lyot coronagraph is shown in Fig. 3(a). Images for vortex coronagraphs having topological charges $m=0$, 1, 2, and 3 are shown in Figs. 3(b)–3(d), respectively. The $m=2$ case provides a bright image of the weak off-axis source, while eliminating light from the on-axis image.

The superior performance of the $m=2$ case is attributed to zero intensity values for the starlight extending over the entire exit pupil of radius R_{EP}. This remarkable result may be found analytically by computing a second-order Hankel transform of the Airy disk.[13] Assuming paraxial rays, we find[19]

$$|U_1(u',v')| = \begin{cases} A_1 R_{\text{EP}}^2/\rho'^2, & \rho' > R_{\text{EP}} \\ 0, & \rho' < R_{\text{EP}} \end{cases}. \quad (5)$$

Equation (5) implies that for $R_{\text{Lyot}} \leqslant R_{\text{EP}}$ the starlight is completely eliminated from the optical system. When the planet and star are well resolved the Airy disk of the planet in plane FP1 will simply experience a negligible tilt owing to the VPM. Hence the planet light is essentially unaffected by the VPM, and image plane FP3 will contain most of the collected planet light. The fraction of transmitted power of a single point source was numerically found to be nearly unity for $\alpha > \alpha_{\text{diff}}$ and to vary as $(\alpha/\alpha_{\text{diff}})^2$ for $\alpha < \alpha_{\text{diff}}$. We note that Eq. (5) may also be obtained by a convolution of the pupil function with the Fourier transform of $t_{\text{VC}}(\theta)$: $r^{-2}\exp(i2\theta)$.

To detect exoplanets, a coronagraph must be able to extinguish starlight that is more than 10 million times brighter than its daughter planet. These cases are numerically challenging. If numerical noise from the bright source has a nonneglible value compared with the weak source signal, then the prediction of Eq. (5) will be difficult to verify. For example, Figs. 4(a) and 4(b) show the cases when $A_1^2/A_2^2=10^6$ and $A_1^2/A_2^2=10^8$, respectively, and $\alpha_2=2.2\lambda/R_{\text{EP}}$. Even in the face of numerical noise both figures demonstrate significant attenuation of starlight (1) and bright high-contrast diffraction-limited images of the planet (2).

One measure of the performance of the coronagraph may be established by calculating the relative power in the final image plane, FP3:

$$\eta = (S_1+S_2)/S_2', \quad (6)$$

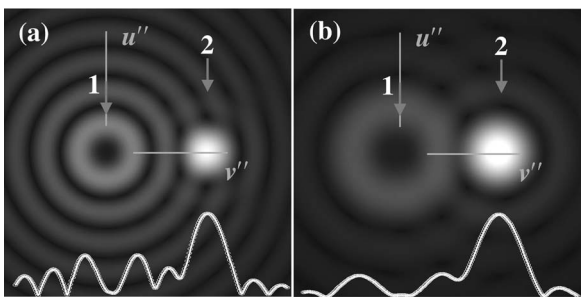

Fig. 4. (Color online) Vortex coronagraph images for the case $m=2$ and $\alpha=2.2\lambda/R_{\text{EP}}$. (a) $A_1^2/A_2^2=10^6$, $R_{\text{Lyot}}/R_{\text{EP}}=0.8$. (b) $A_1^2/A_2^2=10^8$, $R_{\text{Lyot}}/R_{\text{EP}}=0.6$. Field amplitude plots are shown to aid the eye.

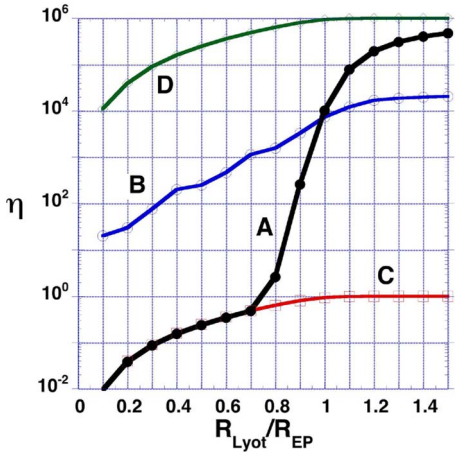

Fig. 5. A, Vortex and B, Lyot coronagraph performance curves for $\alpha=2.2\lambda/R_{\mathrm{EP}}$ where η represents the relative transmitted power. C, Ideal performance. D, Total relative transmitted power without filtering.

where $S_j=\int_{-\infty}^{\infty}\int_{-\infty}^{\infty}|U_j(u'',v'')|^2\mathrm{d}u''\mathrm{d}v''$ is the detected power of the jth source and S_2' is the value of S_2 when $t(\rho,\theta)=1$, $A_1{}^2=0$. A high-contrast image of the planet occurs when $\eta\sim 1$, i.e., where source 1 is extinguished and source 2 suffers no attenuation. Figure 5 shows the performance curve of the Lyot and the vortex ($m=2$) coronagraphs under the condition $A_1{}^2/A_2{}^2=10^6$. The previously assumed parameters were used, except that the optimum configuration for the Lyot coronagraph was assumed[3]: $\alpha_2=2.2\lambda/R_{\mathrm{EP}}$ and $R_{\mathrm{OM}}=3r_{\mathrm{diff}}$. Lines A and B in Fig. 5 indicate the performance of the vortex and the Lyot coronagraphs, respectively, as a function of the relative size of the Lyot stop. Whereas the vortex approach provides excellent results ($\eta\sim 1$) when $R_{\mathrm{Lyot}}\sim 0.8\,R_{\mathrm{EP}}$, the occulting technique of Lyot is unsatisfactory. The theoretically expected value of $\eta=1$ at $R_{\mathrm{Lyot}}=R_{\mathrm{EP}}$ is not expected here owing to our use of soft apertures.

In summary a vortex coronagraph may be designed to completely cancel a diffraction-limited image of a star. The proposed device operates down to the diffraction limit, which is better than the NASA Terrestrial Plant Finding Mission benchmark of $2\lambda/R_{\mathrm{EP}}$. Scattering, aberrations, and the pointing accuracy of a space-based telescope, which are not treated here, are limiting factors. Chromatic limitations of the vortex mask[20] may be overcome using dispersion-compensating techniques.

We thank Johanan L. Codona and Philip M. Hinz. of the Steward Observatory and James H. Burge of the College of Optical Sciences, all at the University of Arizona, Tucson, Arizona, for discussions concerning stellar coronagraphs. D. M. Palacios is now at the Jet Propulsion Laboratory, Pasadena, California. This work was supported by the U.S. Army Research Office and the State of Arizona. G. A. Swartzlander's. e-mail address is grovers@optics.arizona.edu.

References

1. M. A. C. Perryman, Rep. Prog. Phys. **63**, 1209 (2000).
2. F. Roddier and C. Roddier, Publ. Astron. Soc. Pac. **109**, 815 (1997).
3. O. Guyon, C. Roddier, J. Elon Graves, F. Roddier, S. Cuevas, C. Espejo, S. Gonzalez, A. Martinez, G. Bisiacchi, and V. Vuntesmeri, Publ. Astron. Soc. Pac. **111**, 1321 (1999).
4. D. Rouan, P. Riaud, A. Boccaletti, Y. Clenet, and A Labeyrie, Publ. Astron. Soc. Pac. **112**, 1479 (2000).
5. M. B. Lyot, Mon. Not. R. Astron. Soc. **99**, 580 (1939).
6. F. Vilas and B. A. Smith, Appl. Opt. **26**, 664 (1987).
7. J. L. Codona, in Proc. SPIE **5169**, 228 (2003).
8. S. N. Khonina, V. V. Kotlyar, M. V. Shinkaryev, V. A. Soifer, and G. V. Uspleniev, J. Mod. Opt. **39**, 1147 (1992).
9. G. A. Swartzlander, Jr., Opt. Lett. **26**, 497 (2001).
10. J. A. Davis, D. E. McNamara, and D. M. Cottrell, Opt. Lett. **25**, 99 (2001).
11. K. G. Larkin, D. J. Bone, and M. A. Oldfield, J. Opt. Soc. Am. A **18**, 1862 (2001).
12. M. Vasnetsov and K. Staliunas, eds., *Optical Vortices*, Vol. 228 of Horizons in World Physics (Nova Science, 1999).
13. Z. S. Sacks, D. Rozas, and G. S. Swartzlander, J. Opt. Soc. Am. B **15**, 2226 (1998).
14. F. B. de Colstoun, G. Khitrova, A. V. Federov, T. R. Nelson, C. Lowry, T. M. Brennan, B. G. Hammons, and P. D. Maker, Chaos, Solitons Fractals **4**, 1575 (1994).
15. V. V. Kotlyar, A. A. Almazov, S. N. Khonina, V. A. Soifer, H. Elfstrom, and J. Turunen, J. Opt. Soc. Am. A **22**, 849 (2005).
16. J. Sung, H. Hockel, and E. G. Johnson, Opt. Lett. **30**, 150 (2005).
17. E. G. Johnson, J. W. Sung, H. Hockel, and J. D. Brown, "(Domo) Development of 2D phase grating mask using e-beam direct writing for fabrication of analog resist profile," Appl. Opt. (to be published).
18. J. W. Goodman, *Introduction to Fourier Optics*, 2nd ed. (McGraw-Hill, 1996), p. 35.
19. M. Abramowitz and I. A. Stegun, *Handbook of Mathematical Functions*, 9th ed. (Dover, 1970), p. 487.
20. G. A. Swartzlander, Jr., Opt. Lett. **30**, 2876 (2005).